Chalcogenide Letters Vol. 14, No. 9, September 2017, p. 407 - 417

THE FORMATION OF THE MIXED MORPHOLOGY OF NICKEL SULFIDE NANOPARTICLES DERIVED FROM SUBSTITUTED BENZIMIDAZOLE DITHIOCARBAMATE NICKEL (II) COMPLEXES

C. S. THANGWANE, T. XABA[*], M. J. MOLOTO
Department of chemistry, Vaal University of Technology, Private Bag X 021, Vanderbijlpark, 1900, South Africa,

The synthesis of nickel sulfide nanoparticles through variation of reaction conditions such concentration and temperature is reported. Benzimidazole dithiocarbamate nickel(II) and 2-methylbenzimidazole dithiocarbamates nickel(II) complexes were prepared and thermolysed in hexadecylamine (HDA) at the temperature of 140, 160 and 180 °C through the single source precursor method. The effect of concentration of the precursor (0.30, 0.35, and 0.40 g) to produce HDA capped Ni_3S_4 nanoparticles was also investigated. TEM images of the Ni_3S_4 nanoparticles revealed anisotropic particles when the precursor concentration and temperature was varied. 2-methylbenzimidazole dithiocarbamate nickel(II) complex produced the mixture of spheres, cubes, triangles and rods nickel sulphide nanoparticles at different concentrations. XRD patterns displayed the cubic crystalline structures of Ni_3S_4 at all temperatures.

(Received July 9, 2017; Accepted September 29, 2017)

Keywords: Dithiocarbamate complexes (DTC), hexadecylamine (HDA), tri-octylphosphine (TOP), nickel sulfide, nanoparticles

1. Introduction

Nickel sulfide nanoparticles are important family members of the transition metal sulphides nanomaterials. The nickel sulfide nanoparticles have much more complicated phase diagram than the nanoparticles of cobalt sulfide, iron sulfide etc. Their chemical composition comprises of many crystalline phases such as α-NiS, β-NiS, NiS_2, Ni_3S_2, Ni_3S_4, Ni_7S_6 and Ni_9S_8 [1, 2]. Ni_3S_2 crystalline phase has shown a potential application as a low cost counter electrode material in dye induced solar cells [3] while the α-NiS phase has been intensively used as a cathode substance in lithium-ion batteries [4], thermoelectric devices, memory devices [5] and photocatalysts [6].

Nickel sulfide is a p- type semiconductor material with a narrow band gap of 0.4eV. Numerous methods have been used to synthesize NiS nanoparticles such as hydrothermal [7], solvothermal [8], microwave methods [9], and wet chemical methods [10]. Ghezelbash reported the synthesis of Ni_3S_4 nanocrystal through thermal decomposition of $NiCl_2$ and elemental sulphur in oleylamine [11]. A template-promoted growth of NiS nanoparticles was reported by Barry and co-workers [12]. The nanoparticles were grown on anodic alumina templates by decomposing nickel xanthate complex in supercritical CO_2 at 450 °C. Chauhan reported the preparation of $[Ni(S_2CN\ (CH_2)_4CHOH)\ (dppe)]$ as a single-source precursor for the synthesis of nickel sulfide nanoparticles [13].

To the best of our knowledge, $[Ni(S_2N_2C_8H_5)_2]$ and $[Ni(S_2N_2C_9H_7)_2]$ complexes have never been explored and reported as possible single-source precursors for the synthesis of nickel sulfides nanoparticles. In the present work, a simple approach to synthesize Ni_3S_4 nanocrystals via single source precursor method from the prepared nickel dithiocarbamate precursor is reported. The effect of temperature and the concentration variation of the precursor is also evaluated. The FTIR, elemental analysis and TGA were utilized to characterize the nickel complexes and UV-vis, PL, p-XRD and TEM were used to characterize the nickel sulfide nanoparticles.

---

[*] Corresponding author: thokozanix@vut.ac.za

2. Experimental

2.1. Materials and methods

Nickel chloride hexahydrate, trioctylphosphine (97%), hexadecylamine (90%), benzimidazole (98%), 2-methylbenzimidazole (98%), carbon disulphide (99%), sodium hydroxide, toluene (99.8%) and methanol (99.5%) were purchased from Sigma Aldrich and used without any further purification.

2.2 Physical measurements

FTIR spectroscopy was used to study the structure of the dithiocarbamate nickel(II) complex. Infrared analyses were collected on FT-IR Perkin Elmer 400 spectrometer. The spectra were collected over the range from 400 to 4000 cm^{-1}. Elemental analysis was used to check the percentage composition of the complexes. It was carried out in a Leco-CHNS 932 analyzer. About 2.0 mg of complexes were introduced into Ag capsule and placed in a furnace and was maintained at 800 °C using helium as a carrier gas. Thermogravimetric analysis was used to determine the temperature at which the complexes decompose. The sample preparation for thermogravimetric analysis was done by weighing about 13 mg of the complexes. These complexes were decomposed at temperature range of 30 to 900 °C. The analyses were carried out on a Perkin Elmer Pyris 6 manager TGA under an inert environment at a heating rate of 20 $°C.min^{-1}$. UV-vis and PL spectroscopy were used to determine the optical properties of the nickel sulfide nanoparticles. Absorption spectra were measured using a Perkin Elmer Lambda 20 UV-VIS Spectrophotometer at room temperature. The samples were place in quartz cuvettes (1-cm path length) using toluene as a solvent. Emission spectra of the particles were recorded on a Perkin Elmer LS 45 PL spectrometer with a xenon lamp. TEM was used to determine the sizes and morphologies of the nanoparticles. Analyses were done on a LEO JEM 912 electron microscope with an acceleration voltage of 120 KW and a tungsten wire filament. The nickel sulfide samples were prepared by placing a drop of dilute solution of sample in toluene on to a copper grid. The sample was allowed to dry completely at room temperature before the analysis. XRD was measured to reveal the crystalline nature of the nanomaterials on a D8 diffractometer. Samples were placed in silicon zero background sample holder. Measurements were taken using a glancing angle of incidence detector at an angle of 2°using CuKa1 source, for 2θ values over $10^{\circ} – 90^{\circ}$ in steps of 0.05° with a scan speed of $0.01^{\circ}2\theta.s^{-1}$.

2.3. Preparation of dithiocarbamate nickel*(II)* complexes

2.3.1. Preparation of benzimidazole dithiocarbamate nickel(II) complex [Complex I]

A solution of sodium hydroxide (0.78 g, 0.02 mol) which was previously dissolved in 40 ml of distilled water was added into the cold benzimidazole (2.36 g, 0.02 mol) in an ice bath. The mixture was stirred for an hour and carbon disulphide (1.52 ml, 0.02 mol) was added drop-wise and the mixture was stirred for further 12 hrs at 25 °C. A 40 ml solution of nickel chloride (2.37 g, 0.01 mol) was added drop-wise into the corresponding solution of the dithiocarbamate ligand. The mixture was refluxed for 4 hours at 60 °C in a water bath. The reaction mixture was left for few days to crystallize. The precipitate formed was filtered, washed with distilled water and excess methanol and dried in an open air. *The complex was obtained as a green-black coloured precipitate. Percentage yield: 52.63 %. M.pt.216 °C. Elemental analysis (CHNS): Calculated: C, 43.16; H, 2.26; N, 12.58; S, 28.81 %. Found: C, 44.45; H, 2.46; N, 11.88; S, 26.17 %.*

2.3.2. Preparation of 2-methylbenzimidazole dithiocarbamate nickel(II) complex [Complex II]

A 2-methylbenzimidazole dithiocarbamate nickel(II) complex was prepared by the same method as described in section 2.3.1 by using 2-methylbenzimidazole (2.64 g, 0.02mol) instead of benzimidazole. *The complex was also obtained as a green-black coloured precipitate. Percentage yield: 35.88 %. M.pt.212 °C. Elemental analysis (CHNS): Calculated: C, 45.68; H, 2.98; N, 11.84; S, 27.1 %. Found: C, 42.34; H, 2.49; N, 11.25; S, 26.06 %.*

2.4 Synthesis of nickel sulfide nanoparticles

Nickel sulphide nanoparticles were synthesized at different reaction temperatures and different precursor concentrations through single source precursor method. The complex (0.3 g) was dissolved in 5.0 ml of tri-octylphosphine (TOP). The solution was then injected into a hot solution of hexadecylamine (HDA) (6.0 g) in a three-necked flask at different temperatures (140, 160, or 180 °C). The reaction was allowed to stabilize at the desired temperature for an hour. The reaction was then allowed to cool to 70 °C and then the excess methanol was added to flocculate the particles. The black-green nanoparticles were formed and were separated by centrifugation, washed three times with methanol and dried. The procedure was repeated with 0.35 and 0.40 g of the complex instead of 0.3 g at a temperature of 160 °C.

3. Results and discussion

The synthesis of nickel sulfide nanoparticles capped with hexadecylamine using a single source molecular precursor route is investigated. The reaction conditions such as the decomposition temperature and the concentration of the precursor were studied. The dithiocarbamate nickel(II) complexes can be obtained from a reaction of benzimidazole or 2-methylbenzimidazole with carbon disulfide in the presence of sodium hydroxide followed by the addition of nickel chloride. The overall reaction is presented by Scheme 1.

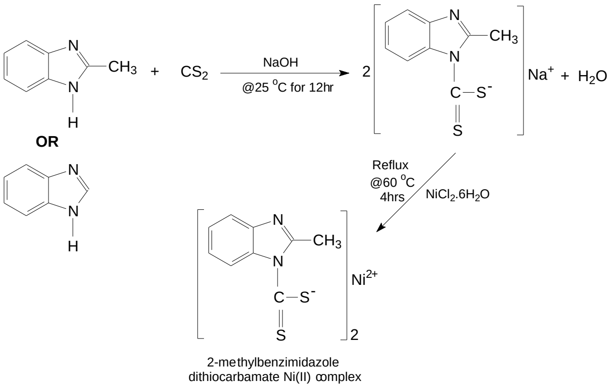

Scheme 1: The preparation of dithiocarbamate Ni(II) complexes

3.1. Spectroscopy and Thermal Analysis

The substances that are formed from the coordination of the metal substances into substituted amines through sulfur atoms in carbon-sulfur group can be used as precursors in the synthesis of metal sulfide nanoparticles [14]. Fig. 1(a) and (b) show FTIR spectra of benzimidazole nickel(II) and 2-methylbenzimidazole nickel(II) complexes. The absence of *v*(N-H) absorption bands at 3116 cm^{-1} in Fig. 1(a) & (b) and the presence of *v*(C-N) and *v*(C=S) weak bands at 1079 and 1034 in Fig. 1(a) and 1085 and 951 cm^{-1} in Fig. 1(b) confirmed the interface between the ligands and metal substances. The presence of *v*(OH) broad absorption band at 3287 cm^{-1} in Fig. 1(a) indicates the presence of water molecules present in the complex. The existence of the stretching bands at 574 and 570 cm^{-1} in Fig. 1(a) & (b) were due to the coordination of the metal with sulfur atoms from the complexes (i.e. M-S) [15]. Table 1 shows the summary of the stretching frequencies from FTIR data.

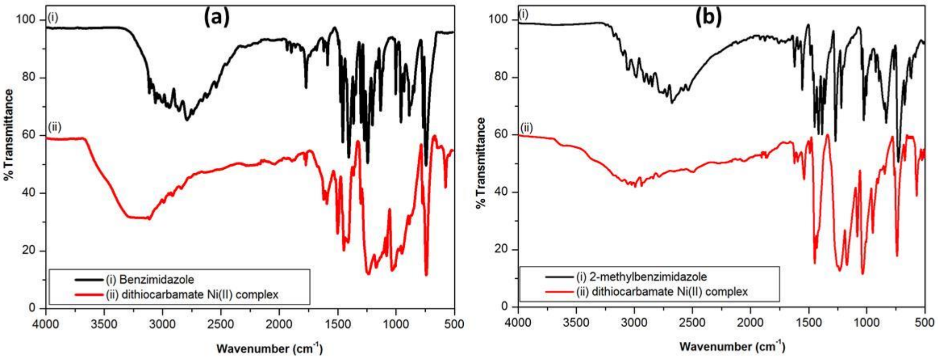

Fig. 1. IR spectra for benzimidazole with complex I (a) and 2-methylbenzimidazole with complex II (b).

Table 1: IR spectral data for complexes I and II

Assignments	**Frequencies cm^{-1}**	
	Complex I	**Complex II**
O-H, Stretching	3287	-
C-N (aliphatic), Stretching	1079	1085
C=S Stretching	1034	951
Ni-S Stretching	574	570

The thermal decomposition of benzimidazole nickel(II) and 2-methylbenzimidazole nickel(II) complexes is shown in Fig. 2. The TGA and DTA curves of complex I (Fig. 2(a)) displayed the first decomposition temperature from 30-135 °C which was due to evaporation of methanol and water. The second decomposition step was due to the loss of benzimidazole molecules from 135-456 °C. The third decomposition step was attributed to the sulfides present in the complex from 541-757 °C. The observed final residue was found to be 39.00 %, which is comparable with theoretical of 40.77 % nickel sulphide (Ni_3S_4). The observed final residue had a mixture of nickel sulphide and nickel as a metal. The TGA and DTA curves of complex II (Fig. 2(b)) revealed two-step decomposition. The decomposition rate was faster compared to the decomposition of complex I (Fig. 2(a)), due to weak Van der Waal's forces between the substituted methyl group and benzimidazole. The first decomposition temperature from 66-135 °C was due to methyl group present in the complex, methanol and water molecules present in the complex. The second decomposition step was due to the loss of benzimidazole molecules and other constituencies present in the complex from 137 °C to 374 °C. The final residue showed a mixture of nickel sulphide and nickel as a metal that was found to be 33.00 %, which is matching the theoretical of 36.14 % nickel sulphide (Ni_3S_4).

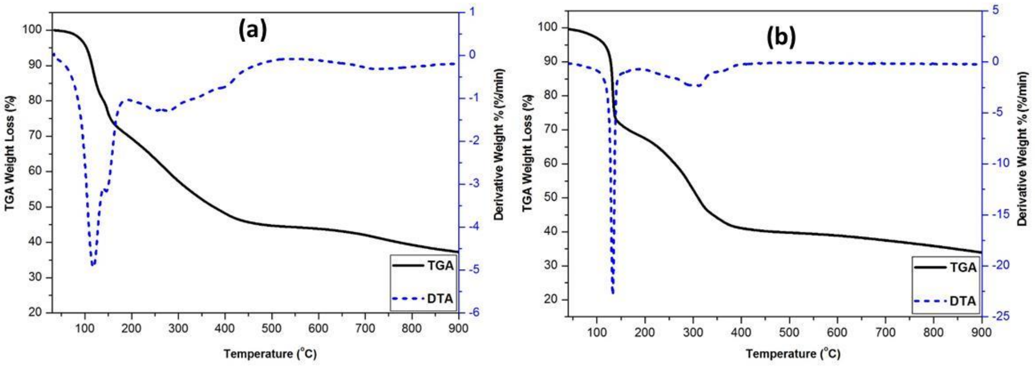

Fig. 2. TGA and DTA curves for complex I(a) and complex II(b)

3.2. Nickel sulfide nanoparticles

3.2.1. Effect of temperature on the formation of Ni_3S_4 nanoparticles from complex II

The absorption spectra together with their corresponding Tauc plots for the nickel sulfide nanoparticles synthesized at different temperatures from complex II are shown in Fig. 3(a) and (b). The absorption spectra of the nickel sulfide nanoparticles in Fig. 3(a) (i) - (iii) are blue shifted in relative to bulk nickel sulfide material (495 nm). It was observed that as the temperature was increased, the size of the particles also increased which could be due to Ostwald ripening effect. The absorption band for the particles synthesized at lower temperature (Fig. 3(a)(i)) was distinctly sharper and more pronounced than the absorption bands of the particles synthesized at higher temperatures. The spectra at high temperatures in Fig. 3(a) (ii) and (iii) show some degree of tailing which is due to the change of shape or the formation of anisotropic particles. The absorption peaks were observed at 360, 365, and 380 nm respectively. The energy band gap values of the NiS nanoparticles can be found by extrapolating the linear part of the plot to $(\alpha h\nu)^2 = 0$. Figure 3(b) shows the optical band gap energies versus the temperature from the obtained spectra. It was observed that as the temperature was increased (Fig. 3(b) (i) - (iii)), the optical band gaps were decreasing and located at 4.35, 4.31, and 4.27 eV.

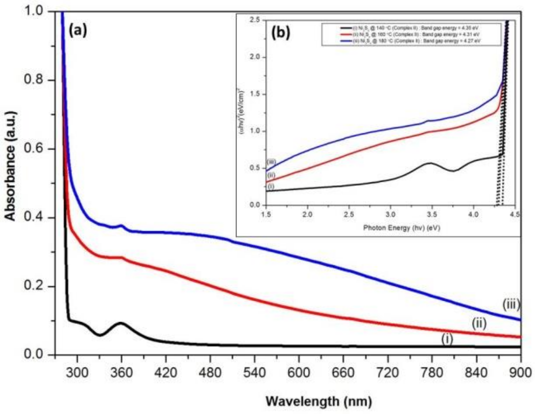

Fig. 3. UV-VIS spectra (a) and Tauc plots (b) of Ni_3S_4 nanoparticles prepared with 0.30 g of complex II at 140 (i), 160 (ii) and 180 °C (iii)

The emission spectra for the nickel sulphide nanoparticles synthesized at different temperatures from complex II are shown in Fig. 4(a) - (c). The corresponding emission spectra were observed with the strong emission peaks centred at 686 nm, 698 nm and 698 nm respectively when excited at 520 nm. The emission peaks were red shifted in relative to the absorption peaks. The broad emission peaks are an indication of a broader size distribution shown by the distribution curves or the presence of anisotropic particles. The emission maxima were slightly shifted towards the higher wavelength as the temperature was increased which is an indication of the formation of the bigger particles.

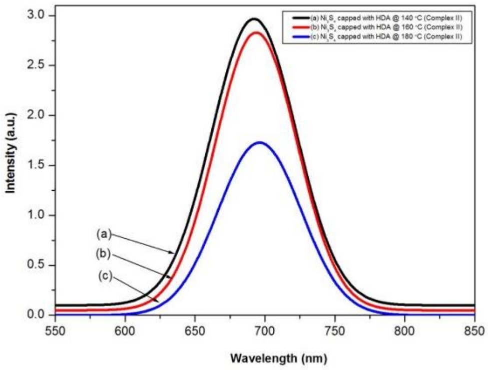

Fig. 4. Emission spectra of Ni_3S_4 nanoparticles prepared with 0.30 g of complex II at 140 (a), 160 (b) and 180 °C (c)

Fig. 5 shows XRD patterns of the particles synthesized at different temperatures from complex II. The peaks between 17 to 25 ° at a lower temperature (140 °C) were attributed to the impurities of C_7OS_8 from the precursor. The peak at 43.96 ° which is indexed to (220) (JCPDS No. 4-835) that corresponds to pure nickel was observed. Five major peaks that correspond to (111), (022), (004), (335), and (137) at 14.85, 26.44, 37.68, 64.30, and 77.51 ° were indexed to the cubic Ni_3S_4. The diffraction peaks matched well with the standard XRD pattern (JCPDS No. 00-043-1469). The wideness of the peaks indicates the presence of smaller particles. The results were similar to the reported by Ji and co-workers [16].

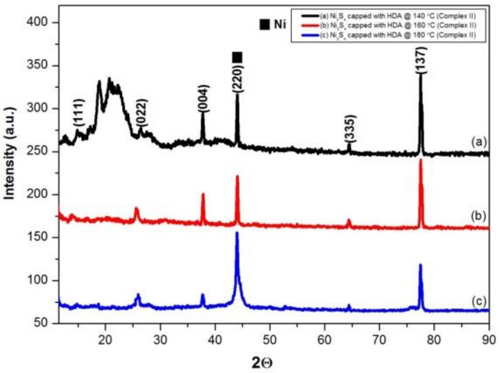

Fig. 5. XRD patterns of Ni_3S_4 nanoparticles prepared with 0.30 g of complex II at 140 (a), 160 (b) and 180 °C (c)

The TEM images of nickel sulfide nanoparticles synthesized from complex II at different temperatures are shown in Fig. 6(a-c). The images show that as the temperature was increased the size of the particles also increased. There was a shape transformation from isotropic to anisotropic shaped particles which is an indication the reaction that favours the kinetic growth regime. There is an evolution of shape from spherical particles to a mixture of cubes, spheres and triangular shaped particles in Fig. 6(a). As the temperature was increased to 180 °C (Fig. 6(c)) the particles became aggregated and the rods like shaped nanoparticles were observed. The estimated average size at 140 °C and 160 °C was found to be 4.21±1.33 nm and 8.86±1.48 nm.

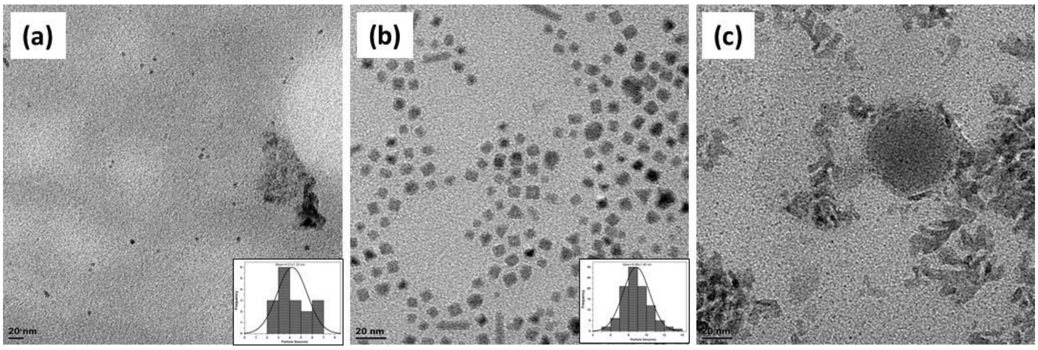

Fig. 6. TEM images of Ni_3S_4 nanoparticles prepared with 0.30 g of complex II at 140 (a), 160 (b) and 180 °C (c)

3.2.2. Effect of concentration of the precursor on the formation of Ni_3S_4 nanoparticles from complex II

The absorption spectra and Tauc plots of nickel sulfide nanoparticles prepared from different amounts of complex II are shown in Fig. 7. The absorption bands (Fig. 7(a)) were blue shifted in relative to the bulk material. The absorption peaks were observed at 360, 357, and 358 nm for the nanoparticles synthesized with 0.30, 0.35 and 0.4 g of complex II. The tailing of absorption spectra was also observed which signifies the presence of particles with different shapes and sizes. The optical band gap energies (Fig. 7(b)) were located at 4.10, 4.23, and 4.21 eV.

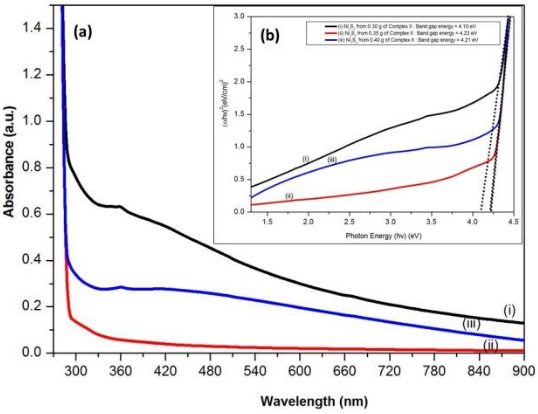

Fig. 7. UV-vis spectra (a) and Tauc plots (b) of Ni_3S_4 nanoparticles prepared at 160 °C from 0.3 g (i), 0.35 g (ii) and 0.4 g (iii) of complex II

The emission spectra of Ni_3S_4 nanoparticles that were synthesized from complex II are shown in Fig. 8(a) – (c). The emission maxima of the samples were red shifted from their respective absorption bands and were observed at 698 nm, 688 nm and 688 nm for the nanoparticles synthesized with 0.30, 0.35 and 0.4 g of complex II at an excitation wavelength of 520 nm. The emission spectra show the broad emission peaks which indicate polydispersity of the particles. The emission maximum shifted towards the lower wavelength at higher concentrations which might be due to change of particle shapes and sizes. The narrow emission peak at low concentration is an indication of smaller particle sizes of nickel sulfide nanoparticles.

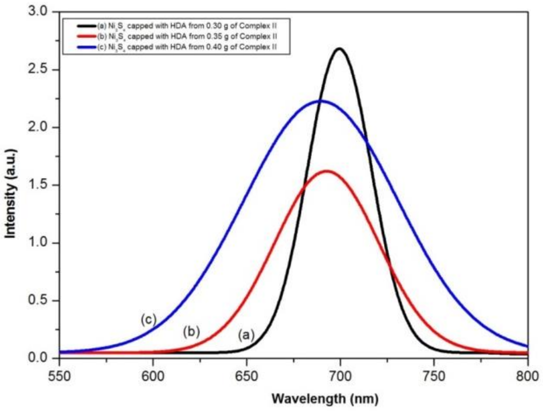

Fig. 8. Emission spectra of Ni_3S_4 nanoparticles prepared at 160 °C from 0.3 g (a), 0.35 g (b) and 0.4 g (c) of complex II

Fig. 9 shows XRD patterns of nickel sulfide nanoparticles synthesized at different concentrations of complex II. At high concentrations, the impurities of C_7OS_8 between 17 to 25° were observed. However at low temperature (Fig. 9(a)), only one peak was observed at 43.69° which is indexed to (220) (JCPDS No. 4-835) that is associated with pure nickel. The main peaks were detected at 15.28, 26.26, 37.81, 64.39, and 77.40° which were indexed to (111), (022), (004), (335), and (137) planes of the cubic Ni_3S_4 (JCPDS No. 00-043-1469). The wideness of the peaks indicates the presence of smaller particles.

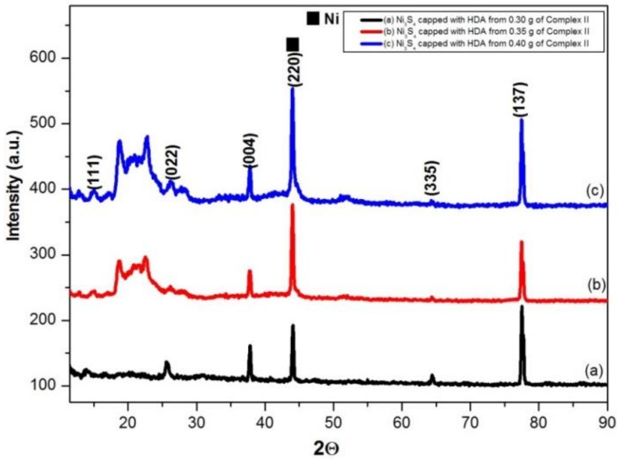

Fig. 9. XRD patterns of Ni_3S_4 nanoparticles prepared at 160 °C from 0.3 g (a), 0.35 g (b) and 0.4 g (c) of complex II

Fig. 10 (a-c) shows the TEM images of nickel sulfide nanoparticles synthesized from complexes II at different concentrations at 160 °C. The images revealed an increase in particle sizes when the concentration of the complex was increased. The TEM images show particles that were dominated with cubes, spheres, triangles and rods-like shaped particles at all concentrations. The particles were well resolved at lower concentration but at higher concentration, the particles were amalgamated to form long rods and bigger cubes particles. The average sizes for the cubes and spheres were found to be 8.86±1.48 nm, 10.26±3.65 nm and 10.42±5.18 nm, respectively.

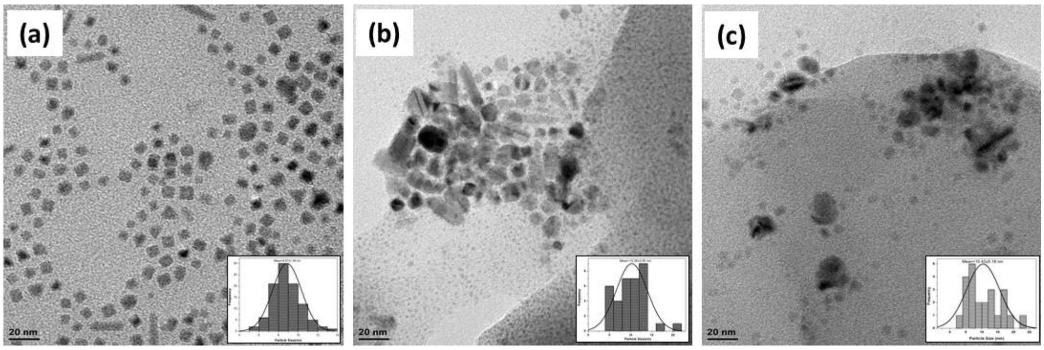

Fig. 10. TEM images of Ni_3S_4 nanoparticles prepared at 160 °C from 0.3 g (a), 0.35 g (b) and 0.4 g (c) of complex II

3.2.3. Effect of precursor on the formation of Ni_3S_4 nanoparticles from complex I & II

Fig. 11 shows the absorption spectra and the Tauc plots for the nickel sulfide nanoparticles synthesized from complex I and II at a constant temperature of 160 °C (Fig. 11 (a)). The spectra show absorption peaks 370 and 365 nm respectively. The optical band gaps in Fig. 11(b) were located at 4.24, and 4.34 eV.

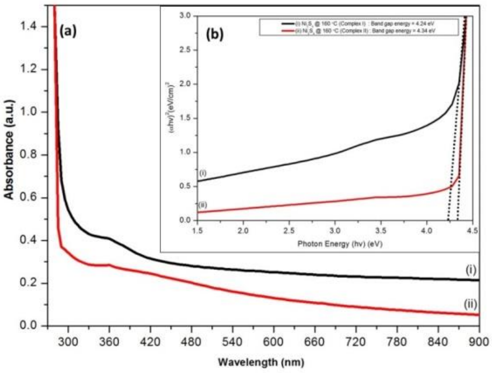

Fig. 11. UV-vis spectra (a) and Tauc plots (b) of Ni_3S_4 nanoparticles prepared at 160 °C from complex I (a) and complex II (b)

The emission spectra (Fig. 12) of the nickel sulfide nanoparticles prepared from complex I and II revealed one strong emission peak that was centred at 698 nm when excited at a wavelength of 520 nm. The sharp emission peaks usually serve as an indication of the narrow size distribution.

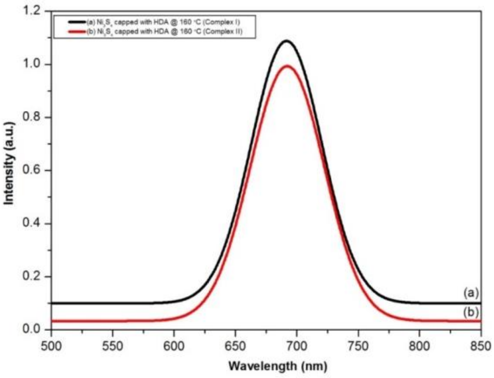

Fig. 12. Emission spectra of Ni_3S_4 nanoparticles prepared at 160 °C from complex I (a) and complex II (b)

The XRD pattern of particles synthesized at 160 °C from complex I and II are represented in Fig. 13. All the spectra show no sign of impurities beside that of the pure nickel at 43.69° which was indexed to (220) (JCPDS No. 4-835). The main peaks were observed at 15.28, 26.26, 37.81, 64.39, and 77.40° corresponding to (111), (022), (004), (335), and (137) planes. The peaks were clearly indexed as the pure cubic phase of Ni_3S_4 (JCPDS No. 00-043-1469).

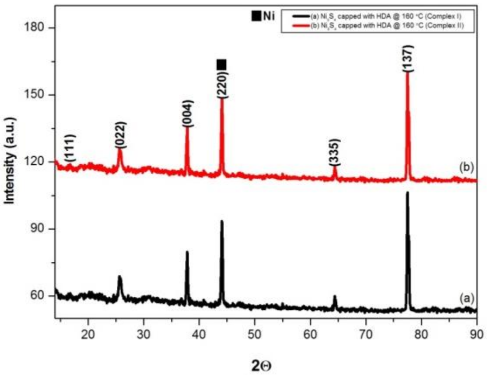

Fig. 13. XRD patterns of Ni_3S_4 nanoparticles prepared at 160 °C from complex I (a) and complex II (b)

The TEM images of particles prepared from complex I and II are shown in Fig. 14. It is clear from the images that spherical nickel sulfde nanoparticles were formed from complex I with an average particles size of 5.813 ± 1.312 whereas the mixture different shapes was observed from the nanoparticles prepared from complex II having average size of 8.86±1.48 nm.

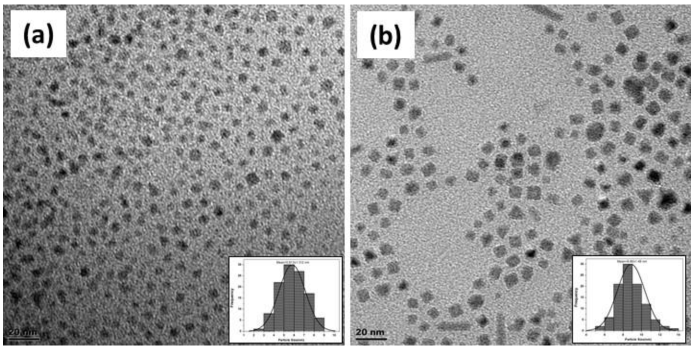

Fig. 14. TEM images of Ni_3S_4 nanoparticles prepared at 160 °C from complex I (a) and complex II (b)

4. Conclusions

Nickel sulfide nanoparticles were synthesized by thermal decomposition of benzimidazole and 2-methylbenzimidazole dithiocarbamate complexes (I and II) in the presence of hexadecylamine as a capping molecule. The optical properties and structural analysis proved that the reaction temperature have an effect on the size and shape of the nanoparticles during the synthetic process. This was confirmed by the increase in the band edges and the change in shape of the nanoparticle prepared when increasing the reaction temperature was increased. The TEM images of nickel sulfide nanoparticles that were synthesized with complex II displayed a variation of anisotropic shaped particles when the decomposition temperature was increased. The concentration of the precursors was also found to have an influence on the synthesis of nanoparticles. Different shapes of nickel sulfide nanoparticles were observed when the amount of the precursor was used to synthesize the nanoparticles. The XRD patterns exhibited cubic phase of

Ni_3S_4 at all temperatures and concentrations. The spectra displayed high impurity factors when the concentration of the complex was increased. The temperature of 160 °C was regarded as the best temperature for the synthesis of Ni_3S_4 nanoparticles since monodispersed and well resolved particles were produced from this temperature.

Acknowledgments

The authors would like to acknowledge the Vaal University of Technology and National research Foundation (TTK13071722088: "Thuthuka Grant Holder") for the financial support.

References

[1] G. Kullerud, R. A. Yund, J. Petrol, **3,** 126 (1962)
[2] C. Sun, M. Ma, J. Yang, Y. Zhang, P. Chen, W. Huang, X. Dong, Sci Rep. **4**, 7054 (2014)
[3] H. K. Mulmudi, S. K. Batabyal, M. Rao, R. R. Prabhakar, N. Mathews, Y. M. Lam, S. G. Mhaisalkar, Physical Chemistry Chemical Physics **13**, 19307 (2011)
[4] S. Han, K. Kim, H. Ahn, J. Ahn, J. Lee, Journal of alloys and compounds **361**, 247 (2003)
[5] M. R. Gao, Y. F. Xu, J. Jiang, S. H. Yu, Chem. Soc. Rev. **42**, 2986 (2013)
[6] Z. H. Chen, P. Sun, B. Fan, Z. G. Zhang, X. M. Fang, J. Phys. Chem. C **118**, 7801 (2014)
[7] C. Xianhui, R. Fan. Chem. Mater **13**, 802 (2001)
[8] H. Wang, J. R. Zhang, X. N. Zhao, S. Xu, J. J. Zhu, Mater. Lett. **55**, 253 (2002)
[9] N. H. Idrisa, M. M. Rahman, S. L. Chou, J. Z. Wang, D. Wexler, H. K. Liu, Acta **58**, 456 (2011).
[10] S. A. Patil, D. V. Shinde, I. Lim, K. Cho, S. S. Bhande, R. S. Mane, N. K. Shresta, J. K. Lee, T. H. Yoon, S. H. Han, J. Mater. Chem. A **3**, 7900 (2015)
[11] A. Ghezelbash, B. A. Korgel, Journal of Langmuir **21**, 9451 (2005)
[12] L. Barry, J. D. Holmes, D. J.Otway, M. P. Copley, O. Kazakova, M. A. Morris, J. Phys Condens Matter **22**, 076001 (2010)
[13] R. Chauhan, M. Trivedi, J. Singh, K. C. Molloy, G. Kociok-Köhn, U. P. Mulik, D. P Amalnerkar, A. Kumar, Inorganica Chimica Acta **415**, 69 (2014)
[14] L. D. Nyamen, A. A. Nejo, V. S. R. Pullabhotla, P. T. Ndifon, M. A. Malik, J. Akhtar, P. O'Brien, N. Revaprasadu, Polyhedron **67**, 129 (2014).
[15] X. L. Yang, G. Q. Zhong, L. Wu, Journal of Chemistry **2013**, Article ID 436090 (2013)
[16] S. Ji, L. Zhang, L. Yu, X. Xub, J. Liu, RSC Adv. **6**, 101752 (2016)